Proceedings of the Sixth International Conference on
Railway Technology: Research, Development and Maintenance
Edited by: J. Pombo
Civil-Comp Conferences, Volume 7, Paper 14.9
Civil-Comp Press, Edinburgh, United Kingdom, 2024
ISSN: 2753-3239, doi: 10.4203/ccc.7.14.9

Analysis of Heat Dissipation of Carbon Ceramic Brake Discs on High-Speed Trains and Its Impact on Surrounding Components Based on Thermal-Solid-Fluid Coupling Method

G. Chen[1], Y. Pan[1], S. Zheng[1], J. Zuo[1,2] and J. Ding[1]

[1]Institute of Rail Transit, Tongji University, Shanghai, China
[2]Shanghai Key Laboratory of Rail Infrastructure Durability and System Safety, Tongji University, Shanghai, China

Abstract

Carbon ceramic brake discs have better performance over the conventional steel brake discs commonly used in high-speed trains. This study analyses the heat dissipation characteristics and their influence on carbon ceramic brake discs. Through FLUENT numerical simulation, the surface temperature of the brake disc and the temperature distribution at different positions of the semi-enclosed space under the vehicle are obtained. The temperature rise of the carbon ceramic disc and the heat distribution law of the carbon-ceramic braking friction pair near the space area under the complex structure of the vehicle are revealed, and the influence of the heat dissipation of the brake disc on the service characteristics and structural safety of the surrounding parts is analysed.

Keywords: high-speed train, brake disc, carbon ceramic, numerical simulation, heat dissipation, temperature distribution.

1 Introduction

The braking system is a key component of railway train safety operations [1]. The basic braking devices of high-speed multiple units currently all adopt disc brakes. The configuration scheme, performance indicators, and heat load capacity directly affect the emergency braking capability of the multiple units [2]. The commonly used steel

brake discs reach temperatures close to 900℃ on the disc surface under emergency braking conditions at an initial speed of 400 km/h. When the braking system works frequently and the thermal stress exceeds the material's strength limit, failures such as thermal cracking and high-temperature deformation may occur in the brake disc [3]. Therefore, there is an urgent need to develop a new type of material for brake discs to meet the development requirements of high-speed and lightweight railway vehicles [4]. Carbon ceramic materials bring better performance to the brake disc itself, such as good thermal stability, minimal wear, stable friction performance, and no thermal fatigue. Currently, researchers are more concerned about the friction and wear performance of carbon ceramic discs as well as their thermodynamic properties [5, 6], while paying less attention to the heat dissipation process of the brake disc during air braking and its effects on the surrounding air domain or other components.

This study employs FLUENT numerical simulation to reveal the temperature rise of carbon ceramic brake discs and the thermal distribution in the vicinity of the friction pair in the complex undercarriage environment of high-speed trains. The aim is to analyse the impact of brake disc heat dissipation on the operational characteristics and structural safety of surrounding components. Firstly, the braking process of high-speed trains is analysed to determine the heat source loading method and boundary conditions, and to compute the braking parameters required for simulation. Then, based on a numerical study of the thermal-solid-fluid coupling system, a thermal-solid-fluid coupling model is established to obtain the surface temperature of the brake disc and the temperature distribution at different positions in the partially enclosed undercarriage space [7]. Lastly, the study summarizes the impact of brake disc heat dissipation on the surrounding temperature distribution and subsequently concludes its influence on the operational characteristics and structural safety of surrounding components.

2 Simulation Methods

Based on the principles of computational fluid dynamics (CFD) and heat transfer, a solid model of the brake disc was established using the spline curve method in SolidWorks, along with a 1:1 typical high-speed Electric Multiple Unit (EMU) train model including the track and train. The mesh was generated using CFD ICEM and imported into FLUENT for numerical calculations to obtain the heat dissipation situation of the uncovered brake disc under emergency braking conditions at an initial speed of 350 km/h. In this study, the uncovered state refers to the absence of skirts on both sides of the bogie compartment in the front of the train. Compared to simulations involving a single brake disc fluid-structure coupling, the model of the front part of the train provides a more realistic representation of the actual working conditions of the brake disc. This is of indispensable importance for studying the heat dissipation characteristics of brake discs in high-speed trains.

2.1 Simulation model

The disc used in this simulation is a carbon-ceramic disc, which differs significantly in structure from traditional brake discs, especially in the area of heat dissipation ribs.

The model of the carbon-ceramic disc is shown in Figure 1. The outer diameter of the carbon-ceramic disc is 670 mm, the inner diameter is 380 mm, and the total thickness is 80 mm. The friction radius of the brake pad ranges from R190 mm to R335 mm. To avoid the influence of boundaries on the flow field around the brake disc, the size of the air domain is set to 10.5 m*7 m*7 m.

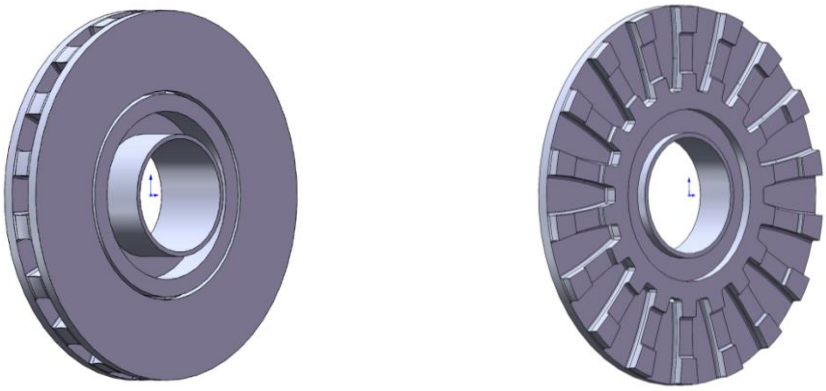

Figure 1: Model of Carbon-Ceramic Disc.

The front part of the train was modelled in 3D using SolidWorks, and a reasonable simplification was made based on the classic EMU model to replicate as closely as possible the real conditions of the aerodynamic braking process for high-speed trains at a 1:1 scale. Considering the symmetrical nature of the front part of the high-speed train, only the front half of the first car of the train was modelled for this analysis. The transient temperature field variation of the first axle disc on the left side of the first bogie (non-powered bogie) of the first car of the train in the forward direction was simulated and analysed. The selected length of the front part of the train is 18m, and the size of the air domain is set to 42 m×25 m×15 m, as shown in Figure 2.

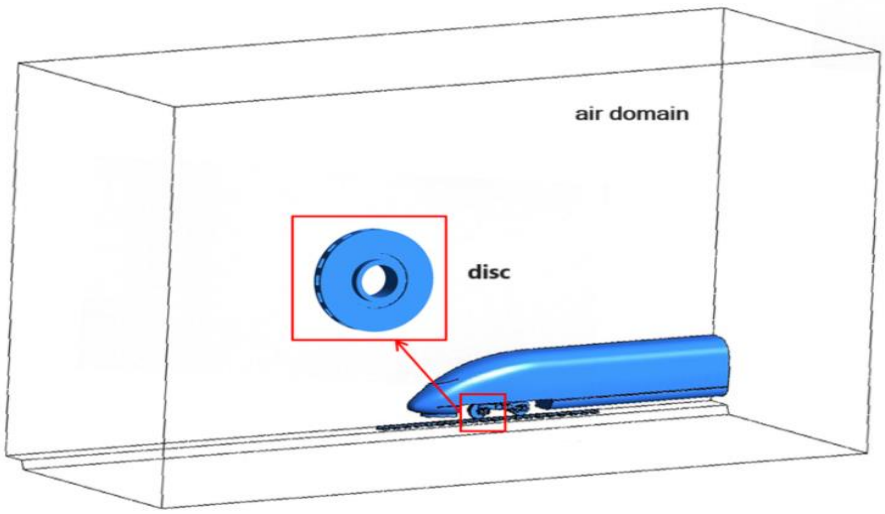

Figure 2: Schematic Diagram of Calculation Region for the Front Part of the Train.

After completing the 3D model of the brake disc and the air domain containing the complex structure of the front part of the train in SolidWorks, the model was meshed using ICEM software. An unstructured mesh type was chosen, with a smaller mesh size near the brake disc and a slightly larger mesh size near the train body surface. Sparse mesh was set further away from the train body surface. Transition zones with appropriate growth factors were used between dense and sparse meshes. The total number of meshes was approximately 2.44 million, as shown in Figure 3.

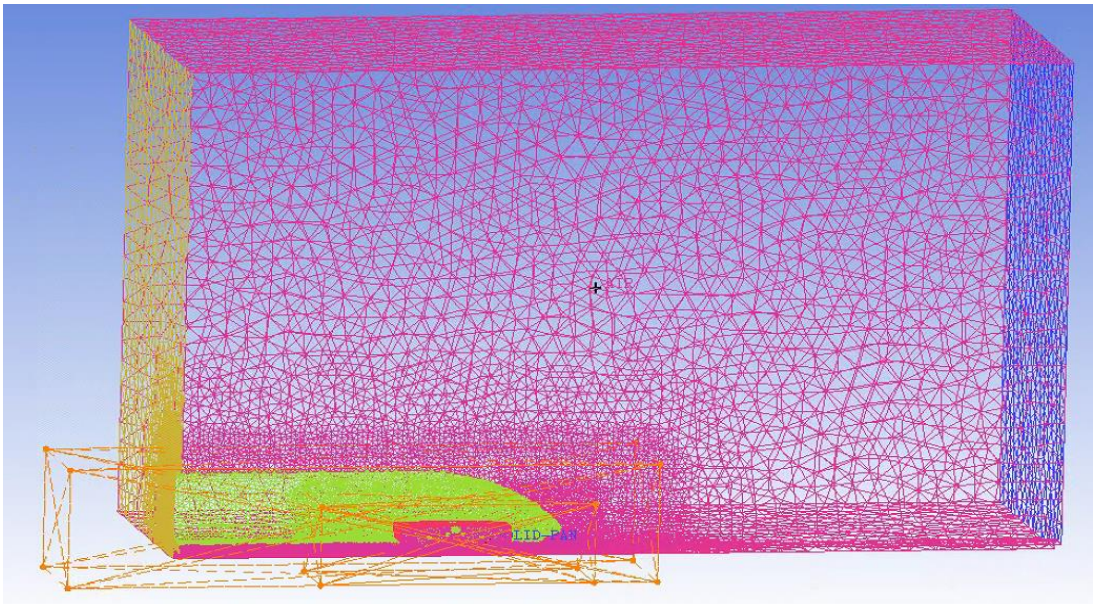

Figure 3: Mesh Model of the Front Part of the Train.

2.2 Simulation parameters and boundary conditions

The material parameters for the simulated carbon ceramic disc are as follows:

Material Properties	Values	Notes
Density	2300 kg/m^3	
Thermal conductivity	85 $W/(m*k)$	Parallel to the friction surface
	40 $W/(m*k)$	Perpendicular to the friction surface.

Table 1: The material parameters for the carbon ceramic disc.

The specific heat capacity of the carbon ceramic brake disc exhibits a trend of initially increasing and then decreasing with temperature. In the simulation setup, this can be achieved by inserting segmented linear functions. The specific values are shown in the table below:

Temperature (k)	373.15	573.15	773.15	973.15	1173.15
Specific heat capacity (J/（kg*k))	800	1300	1550	1700	1600

Table 2: Specific heat capacity of the carbon ceramic disc.

During the braking process, a significant amount of heat is generated. In the simulation of heat dissipation in the brake disc, an incompressible ideal gas model with density varying with temperature can be chosen. The physical parameters of air are as follows:

Specific heat capacity [J/(kg·k)]	Density [kg/m³]	Viscosity [kg/(m·s)]	Thermal conductivity [W/(m·k]
1006.43	Varies with temperature	1.7894e-5	0.0242

Table 3: Physical parameters of air.

The boundary inlet is set as the velocity inlet, with a uniform inflow. The flow direction is along the positive x-axis and has a magnitude equal to the operating speed of the high-speed train.

$$v = v_0 - at \tag{1}$$

The deceleration and braking pressure of the train are as follows in the table:

Speed (km/h)	a_v (m/s^2)	braking pressure (N)
0-120	1.4014	17541.333
120-250	1.2299	17541.333
250-315	1.1025	14352
315-350	0.8624	11162

Table 4: The deceleration and braking pressure of the train.

The outlet is set as a pressure outlet, and the train body and bogie surfaces are all set as non-slip solid wall boundary conditions. A dynamic mesh model (DMM) is employed to set the brake disc solid domain as a rotating region, with the rotational angular velocity equal to the train axle's rotational speed. The interface between the dense air region and the external air domain is set as an "interface" boundary to facilitate data transfer between different domain sections in the computational model. The wall temperature is set equal to the ambient temperature, which is 20°C (293.15K).

Unlike steady-flow materials, in this simulation, the temperature range is significant, causing changes in air density with temperature variation. Therefore, it is necessary to set the direction of gravitational acceleration. The selection of a turbulence model is highly critical for the accuracy of the simulation calculations. In FLUENT, a total of 9 turbulence models are provided. Based on literature research and simulation case analysis, the k-ε model that can be implemented was used in this calculation. During the train braking process, the brake disc converts the train's kinetic energy into thermal energy through friction with the brake pads, thereby reducing the train's speed and achieving the braking purpose. The majority of the heat generated

from friction, apart from a very small portion dissipated directly into the air, enters the brake pads and the brake disc through heat conduction. As the frictional portions of the brake pads on the brake disc are fixed in the radial direction of the brake disc, the input heat flux density varies at different radial positions on the brake disc. This leads to the following formula for input heat flux density:

$$g(v,\ r) = \eta f \cdot \frac{N}{\pi(r_{out}^2 - r_{in}^2)} \cdot \frac{v}{R_{wheel}} r \tag{2}$$

where, r_{out} and r_{in} represent the outer and inner diameters of the brake disc, respectively; v is the real-time running speed of the train; r represents the radius of the position on the brake disc.

The allocation of heat generated by friction during the braking process between the friction pairs is a challenging aspect in establishing a finite element analysis model. Despite various perspectives on this issue, most approaches use a heat distribution coefficient to represent the percentage distribution of heat flux between the friction pairs. Although this heat distribution method ignores the heat transfer generated by friction between the friction pairs, this simulation still adopts this percentage heat distribution approach. In this simulation, the value of η is taken as 0.83.

3 Results

In the emergency braking scenario with an initial speed of 350 km/h, the total time taken from applying the brakes until the train comes to a complete stop is 80.8 seconds. The simulation for the heat dissipation of the brake disc spans from 100 seconds after the start of braking until the end, which includes the entire 80.8-second braking process and the subsequent 19.2 seconds of stationary state. Through the analysis of the simulation results, the temperature rise of the carbon ceramic disc and the heat distribution pattern in the vicinity of the friction pair of the carbon ceramic brake disc under the complex structure of the train will be revealed.

3.1 Analysis of Velocity Field Results

In this study, the analysis of the airflow field is crucial. As shown in Figure 4, the velocity results of the airflow field at two orthogonal and symmetrical sections of the brake disc are extracted for analysis.

Figure 5 shows the velocity contour map of the airflow field in the front part of the train at Section 1. It can be observed from the figure that during the operation of the train, the external air enters the bogie compartment through the position outlined by the red box. Due to the sudden narrowing of the section, the flow velocity increases when the airflow passes through the narrower cross-section, and the velocity decreases after entering the bogie compartment. Figure 6 shows the distribution of flow velocities and streamlines around the brake disc at different time intervals.

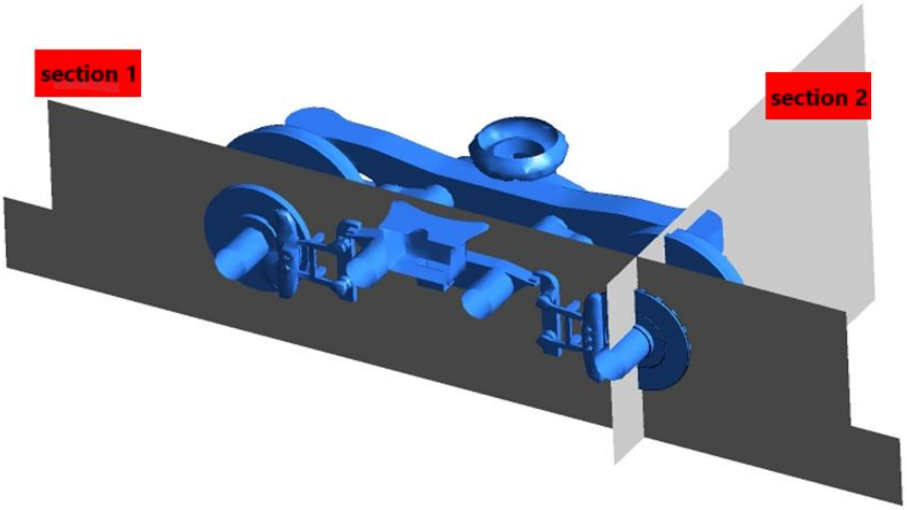

Figure 4: Schematic of the selected section location.

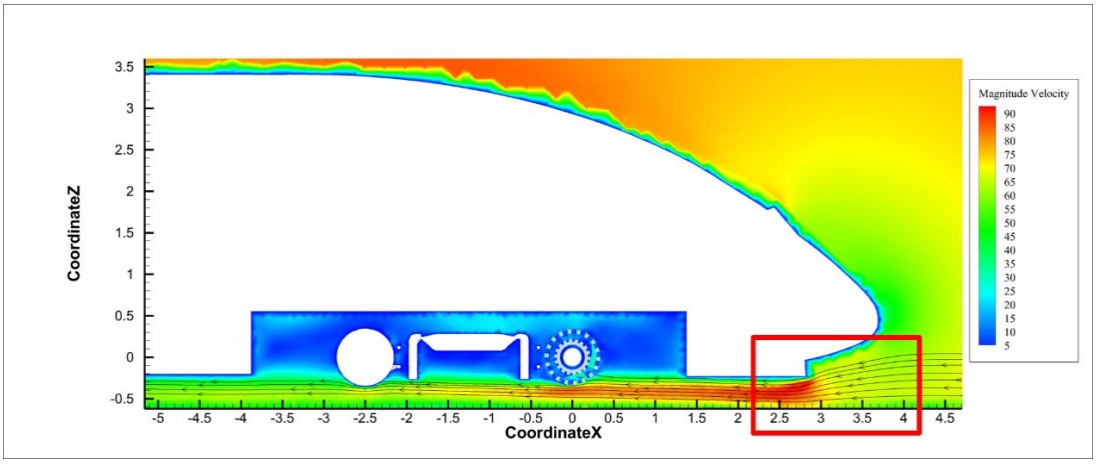

Figure 5: Velocity contour map of the airflow field at Section 1.

During the braking process, as the train moves forward, the airflow around the train exhibits a strong directional flow. The airflow inside the bogie compartment is influenced by both the horizontal motion of the train and the rotational motion of the brake disc. In addition to the complex structure of the internal cooling fins of the brake disc, complex flow phenomena with vortex structures also occur at other locations within the bogie compartment. The airflow becomes turbulent, with significant turbulence energy. The complex structure of the bogie compartment itself is also an important factor contributing to the chaotic airflow within the space. The vortex structures around the brake disc facilitate heat dissipation. Furthermore, the vortex structures near the brake disc can cause negative pressure in multiple areas near the bottom of the bogie, with the most pronounced effect observed in the front of the bogie. For the purpose of this study and due to limitations in length, further elaboration on this topic is not provided here. Observing the streamline map in Figure 6 (e), it

can be seen that after braking, the overall airflow trend is upward. However, due to spatial limitations within the bogie compartment, during the natural convection process, the hot air moves upward while also moving laterally.

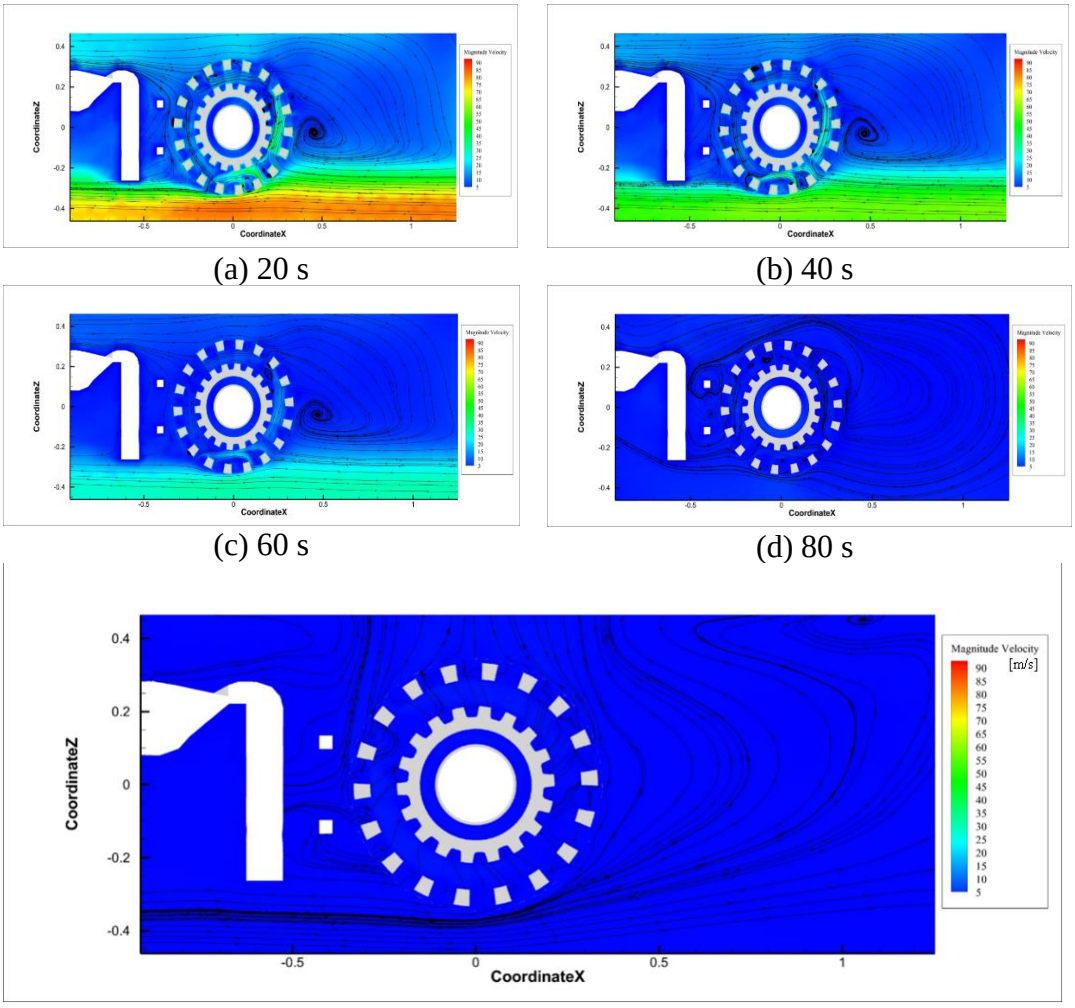

(a) 20 s (b) 40 s

(c) 60 s (d) 80 s

(e) 100 s

Figure 6: Velocity Distribution and Streamline Map of Flow Field around Brake Disc at Section 1.

Figure 7 depicts the velocity distribution and streamline map of the flow field around the brake disc at Section 2 at the 20-second mark. From the figure, it can be observed that the airflow velocity inside the bogie compartment is significantly lower than the surrounding airflow velocity of the train. This effect is particularly pronounced in the upper part of the bogie axle, where multiple vortex structures form on both sides of the axle disc.

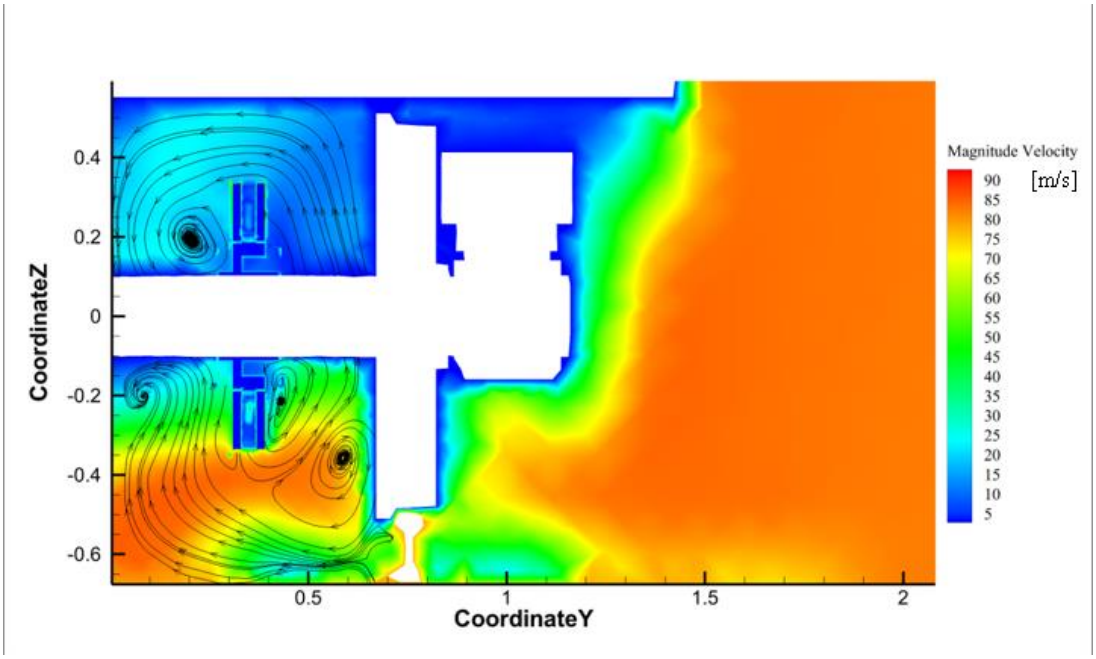

Figure 7: Velocity Distribution and Streamline Map of Flow Field around Brake Disc at Section 2 at the 20-second Mark.

3.2 Analysis of Temperature Field

The simulation results of the temperature field in the locomotive front section can be analysed from two aspects: the solid temperature rise of the brake disc and the temperature distribution in the surrounding air domain. Figure 8(a) shows the curve of temperature variation with radius at different times after the emergency braking is applied to the train. The positions of the selected nodes are 50 evenly distributed nodes along the x-axis at the friction surface of the brake disc.

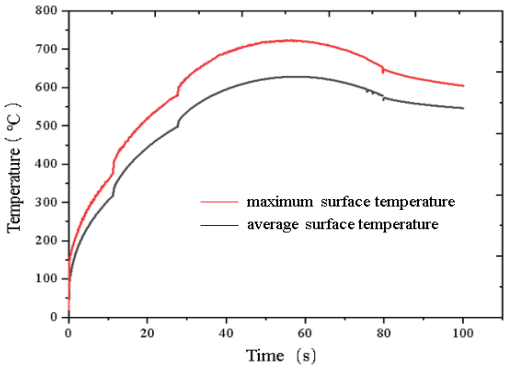

(a) Time variation graph of the disc surface temperature

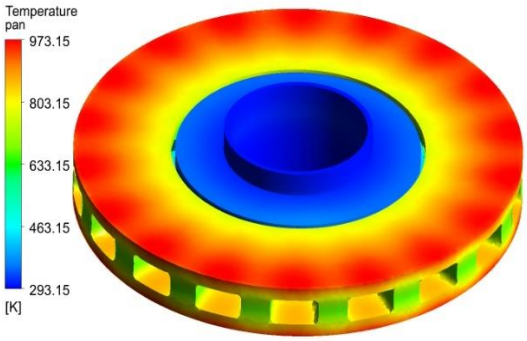

(b) Temperature contour map of the brake disc at 60 seconds

Figure 8: Solid temperature rise of the brake disc.

From Figure 8, it can be seen that the trend of the disc surface temperature curve first rises and then falls. This is because initially the thermal input of the nodes is

greater than the output, and the node temperature rises. When the thermal input and output reach a balance, the node temperature reaches its maximum, and then the thermal input at the node becomes smaller than the output, and the temperature begins to decrease. In this scenario, the highest temperature of 723.81℃ was reached at 55.3 seconds after braking. Analysing the temperature distribution in the air domain around the brake disc inside the bogie compartment, the same cross section as shown in Figure 4 was selected. Figure 9 shows the temperature contour map of the air domain at different times for cross-section 1. Figure 10 shows the temperature distribution and streamline map of the air domain at cross-section 2 at 20 seconds.

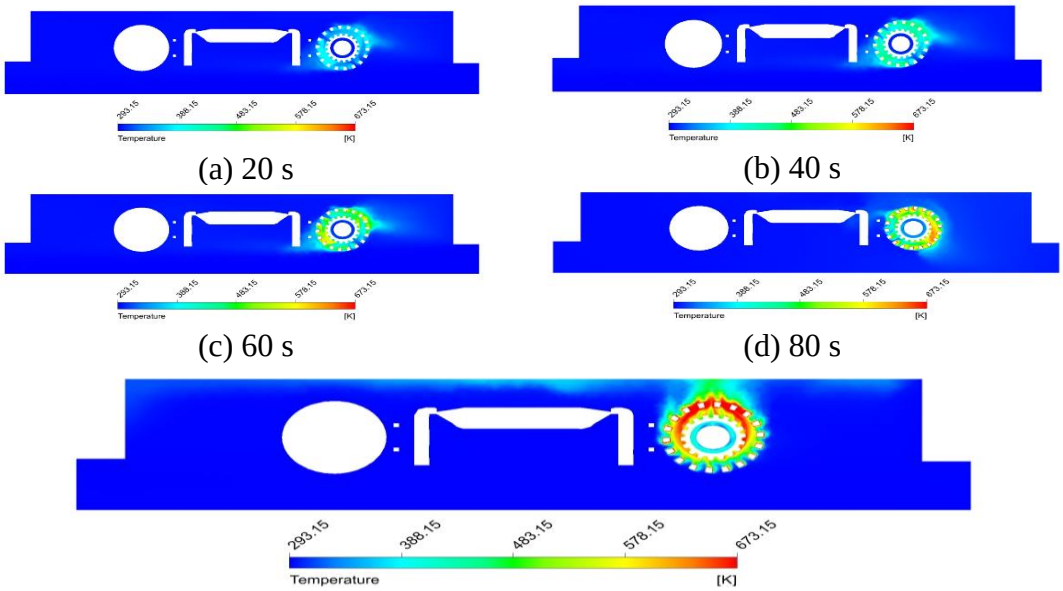

(a) 20 s (b) 40 s

(c) 60 s (d) 80 s

(e) 100 s

Figure 9: Temperature contour map of the air domain at cross-section 1.

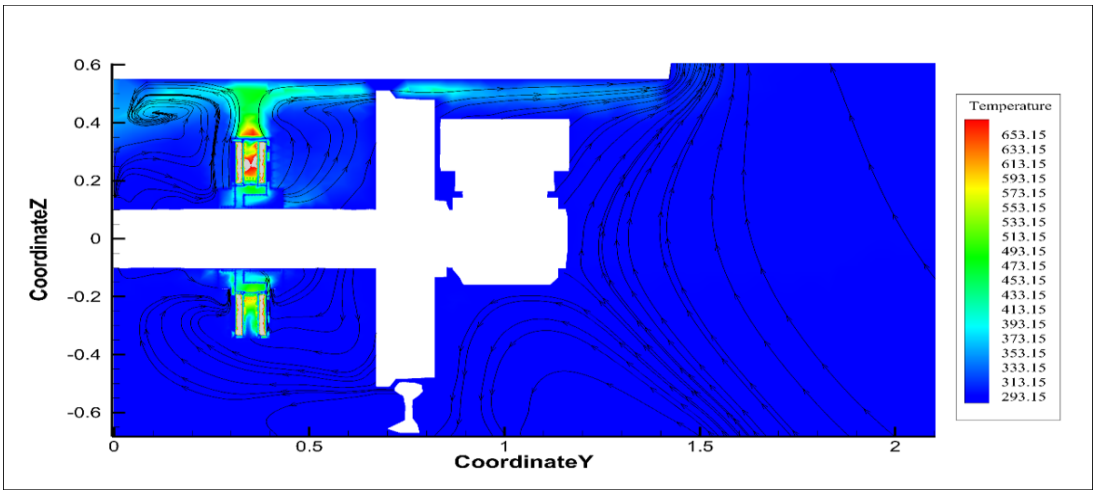

Figure 10: Temperature distribution and streamline map of the air domain at cross-section 2 at 100 seconds.

During the braking process, the air inside the bogie compartment remains in a state of flow, continuously carrying away heat. From the temperature contour maps of the air domain around the brake disc at different times, it can be observed that as the braking time increases, the temperature of the air domain also rises, but only the air temperature around the brake disc shows a significant change. Combining the results of the airflow velocity field simulation in Section 3.1, the temperature distribution in the air domain is not only affected inside the brake disc but also noticeably increases at the exit of the brake disc (i.e., in the direction of the streamlines away from the brake disc). Specifically, the lower left and upper right corners of the brake disc, especially in the vicinity of the vortex structure, exhibit significant heat accumulation.

The convection after the train braking is completed belongs to natural convection, which is different from forced convection. In natural convection, the gas flow is spontaneous. As shown in Figure 10, the air around the brake disc is heated and expands, resulting in a decrease in density and an upward trend.

Take several nodes on the cross-section shown in Figure 4 and output the temperature profiles of these nodes in the air domain. Among them, P10, P2, and P7 are located at distances of 0m, 0.1m, and 0.2m, respectively, from the edge of the brake disc in the vertical direction.

The temperature variation curves with respect to braking time at the locations of nodes P1, P2, and P3 are shown in Figure 12. From the graph, it can be observed that during the braking process, the temperature at nodes P1 and P2 remains relatively constant, while the temperature at node P3 gradually increases due to its proximity to the air outlet of the brake disc. After the completion of braking, the temperature at the nodes fluctuates significantly, but over time, the temperature values gradually stabilize.

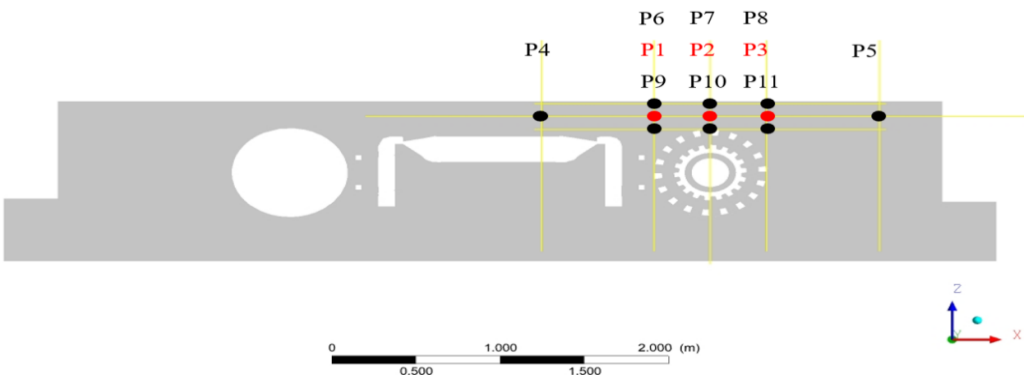

Figure 11: Schematic diagram of the nodes taken at cross-section 1.

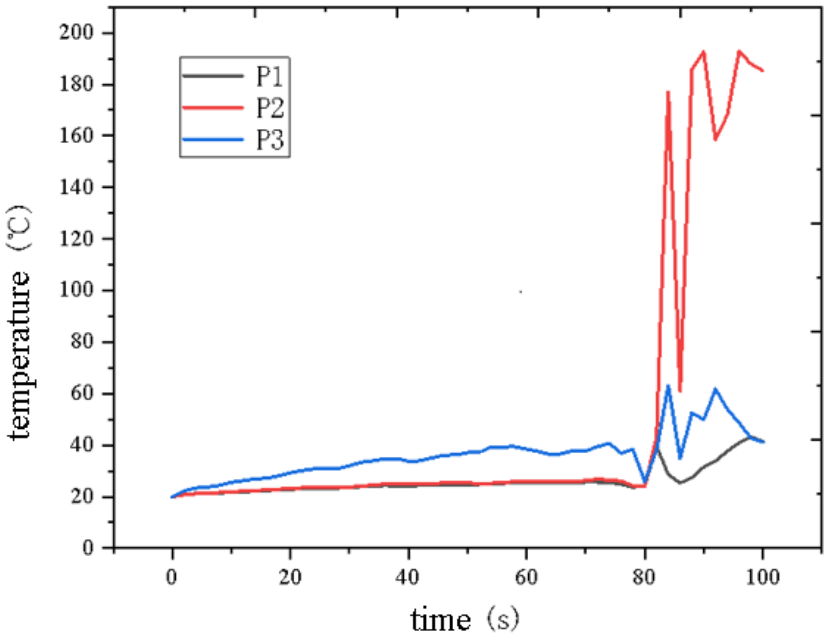

Figure 12: Time-temperature variation graph of nodes.

On the P4-P5 line segment, 100 uniformly spaced nodes were selected to output the time-temperature variation curve of nodes at a distance of 0.1m above the edge of the brake disc when the train applies the brakes for 100s, as shown in Figure 13(a). It can be seen from the figure that the temperature distribution in the air domain above the brake disc is relatively symmetric, with the highest temperature occurring in the middle, reaching a maximum of 238°C.

On the P9-P6, P10-P7, and P11-P8 line segments, 50 uniformly spaced nodes were selected to output the time-temperature variation curve of nodes along the z-axis at the same time as Figure 13(a), distinguished by position 1, position 2, and position 3 from left to right, as shown in Figures 13(c) and 13(d). It can be seen from the figures that at the location directly above the center of the brake disc (position 2), where the brake disc temperature is higher, the temperature in the air domain above the brake disc decreases overall as the distance from the brake disc increases. However, at positions 1 and 3, where the density of hot air is lower, the temperature tends to increase as the height above the brake disc increases.

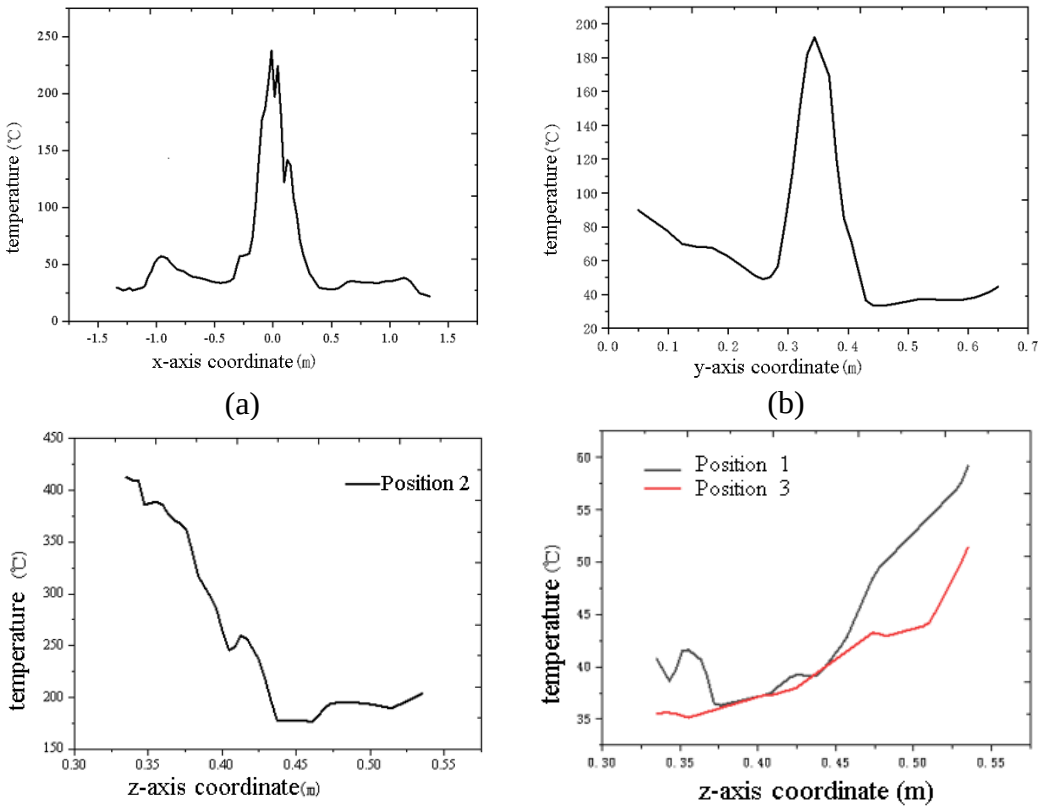

Figure 13: The variation of node temperature with position.

4 Conclusions and Contributions

The study conducts a simulation analysis of the heat dissipation of the brake disc in the unenclosed front part model under the emergency braking condition with an initial speed of 350 km/h. It mainly includes three parts: the velocity field of the surrounding air domain around the brake disc, the temperature field of the solid brake disc, and the surrounding air domain.

(1) Analysis of the simulation results reveals that the front-facing surface of the brake disc experiences a significant reduction in windward area, and the surrounding air flow velocity is generally lower. Furthermore, due to the combined effects of the horizontal motion of the train and the rotational motion of the brake disc, coupled with the complexity of the brake disc and bogie structure, the airflow inside the space becomes turbulent, leading to the formation of multiple vortex structures within and around the brake disc.

(2) The friction surface temperature of the brake disc initially increases and then decreases over time. The node temperature, on the other hand, generally increases with increasing radius but decreases near the outer edge of the brake disc. In this particular scenario, the highest temperature of 723.81℃ is reached at the moment when 55.3 seconds have passed after the brakes are applied.

(3) At the moment when the train applies brakes for 100 seconds, the node temperature in the air domain located 0.1m above the edge of the disc exhibits a nearly symmetrical distribution along the x-axis direction. The highest temperature at the central position reaches 238℃.

Acknowledgements

The authors would like to appreciate the funding support from the National Natural Science Foundation of China (Grant No. 62273258), Science and Technology Research and Development Programme Topics of China State Railway Group Co., Ltd. (Grant No. K2023J005), and the Fundamental Research Funds for the Central Universities (Grant No. 22120240183).

References

[1] B. Ghadimi, F. Kowsary, M. Khorami, “Thermal analysis of locomotive wheel-mounted brake disc”, Applied Thermal Engineering, 51(1-2), 948-952, 2013.

[2] H. Sheng, Z.H. Wang, J. Shao, K.C. Qian, Z.H. Zhou, S.Z. Wu, "Research Status and Prospect of Brake Dise Materials for High-Speed Train", Materials for Mechanical Engineering, 40(01), 1-5, 2016.

[3] S.X. Zhou, X.H. Zhao, C.L. Sun, Y. Sun, "Prediction of Crack Propagation Life of Cast Steel Brake Disc of EMU", Journal of Mechanical Engineering, 54(24),154-159, 2018.

[4] S.T. Zhu, F. Wang, H.Q. Chen, Y. Liu, "Research Status of Brake Disc Steel for High-speed Train", Foundry Equipment and Technology, 02, 62-66, 2023.

[5] F.F. Qian, L.B. Zeng, Y.J. Shi, W.W. Jin, Y.S. Meng, "Research of C/C − SiC brake discs for high speed EMUs", Materials for Rail Transportation System, 2(03), 11-16, 2023.

[6] C. Yang, F. Qiao, F.L. Yao, W.L. Yu, X.J. Shi, Y.P. Wang, "Characteristics of C/Ceramic brake discs and their application in rail vehicles", Materials for Rail Transportation System, 2(06), 10-13, 2023.

[7] S.Z. Zheng, J.X. Ding, J.Y. Zuo, “Research on heat dissipation of brake disc in the semi-enclosed space under high-speed train based on fluid-solid-thermal coupling method”, Case Studies in Thermal Engineering, 56, 104295, 2024.